Project Narrative

Introduction

The advent of x-ray free electron lasers (xFELs) has brought the ability to resolve ultrafast processes in molecular and material systems on their natural time and length scales [1–4]. The requisite synchronization of x-ray pulses to optical pulses has remained challenge central to xFELs since their inception [5–15]. At the Linac Coherent Light Source (LCLS), 120 Hz recording for area detectors has allowed a measure-and-sort paradigm for correcting the 100 fs rms residual timing jitter to better than 10 fs rms [11–13]. Given the MHz scale repetition rate of Table 1 for the coming facility upgrade — the Linac Coherent Light Source II (LCLS-II) — such a measure-and-sort method would effectively require every shot be recorded, increasing the data load from the 10 TB/day of today to 100 PB/day. Such a load would require an enormous cost for developing the ultra-high duty-cycle area detectors and the corresponding network and storage infrastructure. For the reproducible samples such as gases, solutions, or damage resistant crystals typical of x-ray FEL experiments, multi-shot averaging detectors are a much preferred and enormously cheaper solution, although they preclude the measure-and-sort paradigm. We propose a research program aimed at $\geq$ 100 kHz repetition rate, x-ray/optical cross-correlation technique, with better than 10 fs resolution that can serve as feedback for an improved synchronization system, thus enabling high time-resolution multi-shot averaging experiments at LCLS-II.

Many attosecond scale experiments, currently only enabled by high-harmonic generation (HHG) [17–20], would greatly benefit from the much higher brightness of an attosecond xFEL beamline [21, 22]. This would effectively exchange the flux challenge of HHG sources for the challenge of synchronizing optical and xFEL pulses with 100 attosecond precision. We propose a two-dimensional spectrogram approach [23] to improve the temporal resolution of x-ray/optical cross-correlation techniques to $\sim$100 attoseconds. Such a method would enable measure-and-sort correction of the residual temporal jitter, enabling attosecond science at LCLS for $\geq$10 kHz repetition rates limited only by the on-board processing of the two-dimensional spectrogram images.

Table 1: Soft x-ray conditions for LCLS-I and the high-repetition rate LCLS-II. [16]

Parameter	LCLS-I	LCLS-II
Max rep. rate	120 Hz	930 kHz
Average power	0.5 W	200 W
Pulse energy	4 mJ	0.1–5* mJ
Photon energy range	0.25–2 keV	0.2–5 keV
Bunch arrival time stability	100 fs rms	20 fs rms

* $\geq$ 200 μJ only at reduced repetition rate, conserving 200 W maximum average power.

Achieving the full capability of x-ray laser science will require the control of the x-ray spectral phase. The development of temporally shaped x-ray FEL pulses would not only facilitate attosecond pulse generation but also a number of multi-pulse non-linear techniques. A continued progress on this front [24–30] will require full spectral phase, amplitude and polarization characterization. We therefore propose a single-shot diagnostic that reports the full temporal intensity, wavelength, and polarization distributions with $\sim$150 attoseconds resolution at $\geq$10 kHz repetition rates, again limited only by the on-board processing of effectively two-dimensional signals.

The area of ultrafast timing and synchronization is very broad and requires developments on many fronts. This proposal addresses a targeted, self-contained, subset — cross-correlation measurement and analysis — consistent with the scope of an Early Career award. We restrict ourselves to three fundamental objectives:

1. Developing a $\geq$100 kHz repetition rate x-ray/optical cross-correlation technique, fed back into the laser synchronization system, to maintain 10 fs rms temporal stability for multi-shot averaging experiments at LCLS-II.
2. Extending the x-ray/optical cross-correlation technique to allow for single-shot sorting of the residual jitter to a resolution of $\sim$100 attoseconds at a $\geq$10 kHz repetition rate.
3. Developing a single-shot diagnostic that reports the full temporal intensity, wavelength, and polarization distribution also with $\sim$150 attoseconds resolution at a $\geq$10 kHz repetition rate.

Objective 1 – Femtosecond jitter control

We propose a research program aimed at a matched high repetition rate x-ray/optical cross-correlation measurement that feeds results directly into the timing and synchronization system in order to fully capitalize on the short pulses of the LCLS-II [16]. The precise synchronization of x-ray free electron lasers (xFELs) with optical lasers has been a fundamental challenge since the early days of the Sub-Picosecond Photon Source (SPPS) at SLAC [5] and the Free-Electron Laser at Hamburg (FLASH) [6, 7]. Currently at SLAC, the experimental lasers are synchronized to an rf distribution while an all-optical distribution is used at FLASH [31]. In both schemes the x-ray pulse is only indirectly locked by measuring an optical readout of an electro-optic (eo) signal produced by the electron bunch in much the same fashion as the decade old method of Ref. [5]. Although the $\sim$100 fs rms residual jitter at LCLS is largely due to electron bunch energy variations, the state of the art residual jitter of $\sim$20 fs in Ref. [31] is primarily due to the variation of the lasing process along the electron bunch. This drives our need for a direct measurement of the x-ray pulse itself.

The idea of a direct cross-correlation does not simply transfer from the optical to the x-ray regime. In the optical regime, one typically uses the $\chi^{(3)}$ nonlinear susceptibility to imprint the intensity distribution of an unknown pulse onto a known readout pulse. There is a negligible $\chi^{(3)}$ mediated interaction in the x-ray regime; the x-ray pulse predominantly couples to the optical field by the linear x-ray absorption induced hot carriers which subsequently thermalize over the course of about 30 fs [32]. The $\sim$30 fs thermalization, a fundamental temporal blurring, is a general property of dielectrics and a characteristic timescale of radiation damage [33]. We will reserve our discussion of instantaneous gas-phase photo-electron streaking for Objective 3. Despite its temporal blurring, x-ray-induced carrier cascade is the most widely used phenomenon for timing at xFELs [6–15].

Traditionally, a short optical pulse is geometrically crossed with the x-ray pulse in a condensed medium such that the crossing angle provides a time-to-space arrival-time mapping [6–9, 14, 15, 34]. The typical 45° crossing angle and 1 mm spot size gives a temporal window just over 2 picoseconds. Besides the blurring from the carrier cascade, the timing resolution is predominantly determined by the pulse durations and the imaging resolution of the optical lens system. In practice, such spatial encoding gives about 50 fs rms resolution when used for sorting the temporal jitter [8, 9].

Seeing the practical limitations to spatial encoding, we merged an earlier concept based on chirped pulses [35, 36] with the materials mediated interaction paradigm to pioneer an alternative approach depicted in Fig. 1 [10–13]. In spectral encoding, a small portion of the primary optical pulse is split away from the main beam and focused into either a pressurized gas cell or a sapphire plate. The short pulse then forms a stable filament that strongly modulates the input spectrum to produce an output spectrum that spans the entire visible spectrum [37]. We pass the resulting supercontinuum pulse through up to 1 cm of glass for a group delay dispersion (GDD) of over 10^3 fs^2. This chirped supercontinuum exhibits a smoothly monotonic delay-to-wavelength mapping within the active 450 nm – 650 nm spectral region with a 2 ps temporal window similar to the spatial case. The chirped supercontinuum is then overlapped with the x-ray pulse in the interaction medium, typically Si_3N_4 or Ce:YAG crystals. For the normal material dispersion, as indicated in Fig. 1, the early arriving red end of the spectrum passes unaltered through the material before the x-ray pulse arrives. The late arriving blue part of the spectrum arrives after the x-ray pulse and therefore experiences the modified optical transmission. The spectral location of the abrupt change in transmission then indicates the arrival time of that particular xFEL shot.

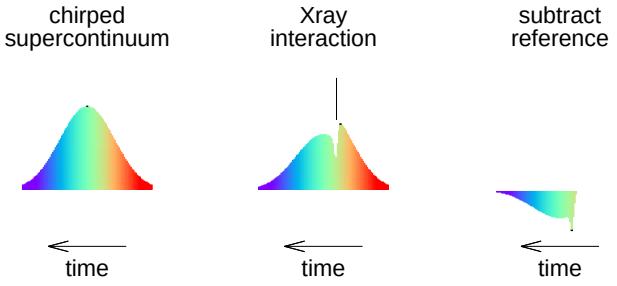

Figure 1: Normal, non-interferometric spectral encoding [10–13]. The supercontinuum pulse spans the visible spectrum and is chirped under normal dispersion such that the red end of spectrum arrives early while the blue end arrives late. When an x-ray pulse intercepts the middle the pulse in a transparent dielectric material, the optical transmission is reduced for all colors that arrive after the x-ray pulse. The "head" of this depletion edge indicates the arrival time of the x-ray pulse.

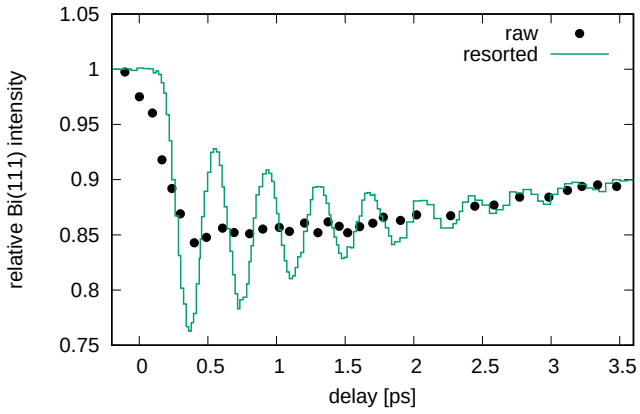

Figure 2: Raw (black dots) and sorted (green steps) x-ray Bragg scattering from Bismuth (110) versus ir pump pulse delay [12]. The clear oscillation features exemplify the advantage of measure-and-sort jitter correction for time-resolved x-ray science.

The resolution in our spectral encoding method is primarily determined by the spectral support bandwidth that is present in the medium while the hot carriers cascade and thermalize. The spectral resolution of our typical 1/2 m spectrometer is well below 1 nm and so the time-bandwidth product of the carrier response plays the largest role in determining the sharpness of the spectral edge feature in Fig. 1. This resolution can be improved, a smaller required delay window needs less chirp and therefore provides more bandwidth per unit time, in turn supporting a sharper edge [13]. In practice, our time-sorting resolution ranges from 5 fs rms [11, 13] to about 20 fs rms [12] depending on this supercontinuum chirp. Figure 2 shows typical unsorted data (points) versus the spectral encoding based time-ordered histogram (lines) for x-ray Bragg diffraction (110) from optically pumped phonons in Bis-

muth.

Since spectral encoding provides streaming real-time sorting, users now often use spectral encoding in combination with an artificially introduced asynchronous oscillation in the delay. Effectively worsening the synchronization to well above 500 fs rms allows for a quasi-stochastic sampling of the entire delay range, equally building up statistics over the temporal window of interest. Alternatively, users manually paint the statistics over delay regions, lingering in regions while interesting time-dependent features emerge. This ability to sort quasi-stochastic delays relies entirely on all detectors running at the full beam rate. Many experimental techniques that rely on area detectors will require averaging many 930 MHz shots per image frame, precluding the current single-shot time-sorting of the 120 Hz LCLS.

The benefit of fast and manual scans over relevant delay windows coupled to the need for multi-shot averaging drives our motivation for a very high repetition rate x-ray arrival time monitor for LCLS-II. By directly measuring the x-ray arrival time with spectral encoding, and then feeding that measurement directly into the optical laser synchronization system, we would enable sub-10 femtosecond resolution even in multi-shot averaging experiments. Such an integrated synchronization system could be programmed to add an arbitrary oscillation, constrained to lower frequency than the detector readout rate, that distributes statistics over a desired window. More importantly, the nonlinear x-ray science proposed for LCLS-II [16] could uniquely leverage the high repetition rate by using a controlled modulation of the delay in order to produce lock-in amplification of weak delay dependent signals. Given the predominance of x-ray background over the expected weak signals, time-domain lock-in amplification would leverage the continuous 930 kHz pulses that are unique to the LCLS-II. We will therefore research an x-ray optical cross-correlation scheme that provides real-time sub-10 fs rms results for use in the synchronization feedback loop at high repetition rate.

There are significant challenges to transferring spectral encoding to the LCLS-II, the most pressing of which is the required x-ray dose per shot for healthy signal to noise ratios. Typical signal levels of 30% require absorbed dose levels as high as 200 μJ in a 1 mm spot size. From LCLS to LCLS-II, the current 24 mW deposition would need to increase to nearly 200 W of deposited power. Clearly a more sensitive scheme is needed that requires much less x-ray dose. Many x-ray-opaque condensed phase experiments require an upstream arrival time measurement and thus a measurement largely transparent to the x-ray beam. Again, the absorbed dose in this case must be kept to a small fraction of the incident photons. Ideally the arrival time computation must be performed on-board of the detector in order to minimize the amount of network traffic for the synchronization. The three principle challenges to delivering high time resolution to LCLS-II are therefore:

1. The required dose for acceptable signal-to-background must remain low enough that the target material can either survive the high average power of the LCLS-II machine or it can be continuously refreshed.

2. Appreciable signals should be achievable with very thin, x-ray transparent, samples in order to make the measurement upstream of the experiment or else used with an e.g. alternate order from a monochromator grating as at SACLA [14, 15].

3. The analysis algorithm must occur on-board of the detector to reduce network data transfer and be made available to the laser synchronization system for $\geq$1 kHz feedback control.

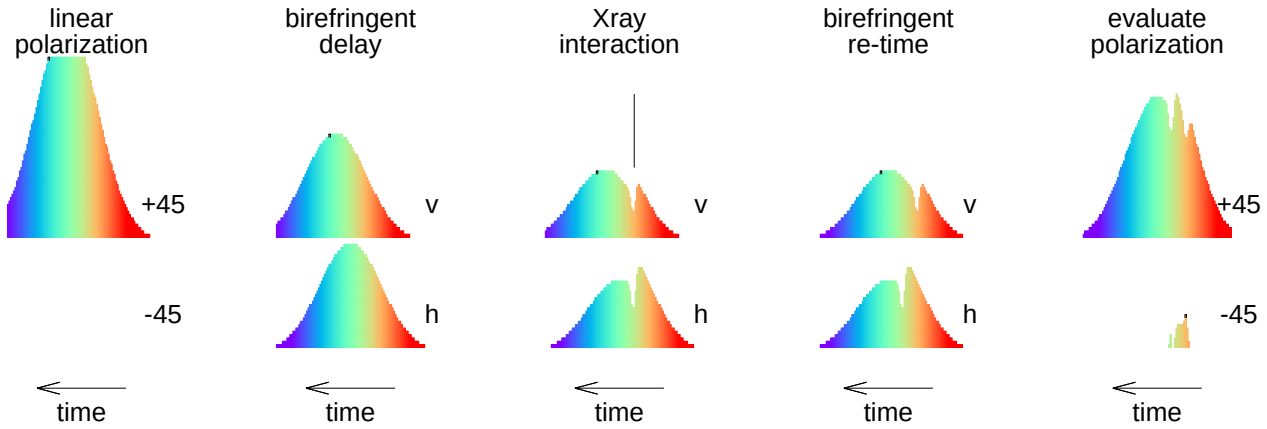

Figure 3: Schematic of one-dimensional interferometric spectral encoding. As in normal spectral encoding (Fig. 1), normal dispersion causes the red end of the visible spectrum to arrive early, the blue end late. We use a birefringent delay between two different polarizations so that the depletion of the spectral transmission occurs are different relative time delays for the two polarizations. After the x-ray interaction, we re-time the polarizations with a matched birefringent plate. This offsets the spectral depletion features and this offset region then exhibits a polarization rotation. The rotated component is then isolated with a downstream polarizer before being measured in a spectrometer.

We plan to address the first two requirements with an interferometric extension of spectral encoding along with an exploration of novel materials and the last requirement with optimized on-board data processing.

As depicted in Fig. 3, we propose to bring interferometric sensitivity to the spectral encoding method [10, 12, 13]. In interference mode, partly inspired by Ref. [36], a birefringent plate splits a $45°$ polarized supercontinuum pulse into vertical and horizontal polarized components with 100s of femtoseconds of relative delay. The cross-polarized yet co-propagating pulses can then be overlapped with the x-ray pulse at the interaction medium, e.g. Si_3N_4 or liquid water sheets. After interaction, the pulses will be re-timed with a matched birefringent plate in orthogonal orientation. Upon re-timing, a crossed $-45°$ polariser will completely reject all wavelengths except those spectral components that arrived before the x-ray pulse for one polarization but after for the other pulse. The transmitted spectrum through the crossed polarizer serves as the interferometric spectrally encoded x-ray arrival measurement.

Polarization management critically determines the sensitivity for interferometric spectral encoding. The more purely we maintain our polarizations, the higher we can push the efficiency of continuum generation; the more continuum we have for input, the less absorbed x-ray dose needed to get a measurable signal through that crossed polarizer. The traditional sapphire-based supercontinuum is far too weak for our cross-polarized interference technique while photonic crystal fiber continuum exhibits a high-order phase modulation that precludes a smoothly monotonic spectrum-to-time mapping. We therefore choose to generate the supercontinuum with a pressurized gas cell [23] for the sake of a high brightness filament that produces a white light pulse with low-order polynomial phase. Preliminary results are shown in Fig. 4 for both soft and hard x-ray interactions. Moving forward, we will explore both hollow-core capillary and a multi-plate geometry [38] in order to achieve as

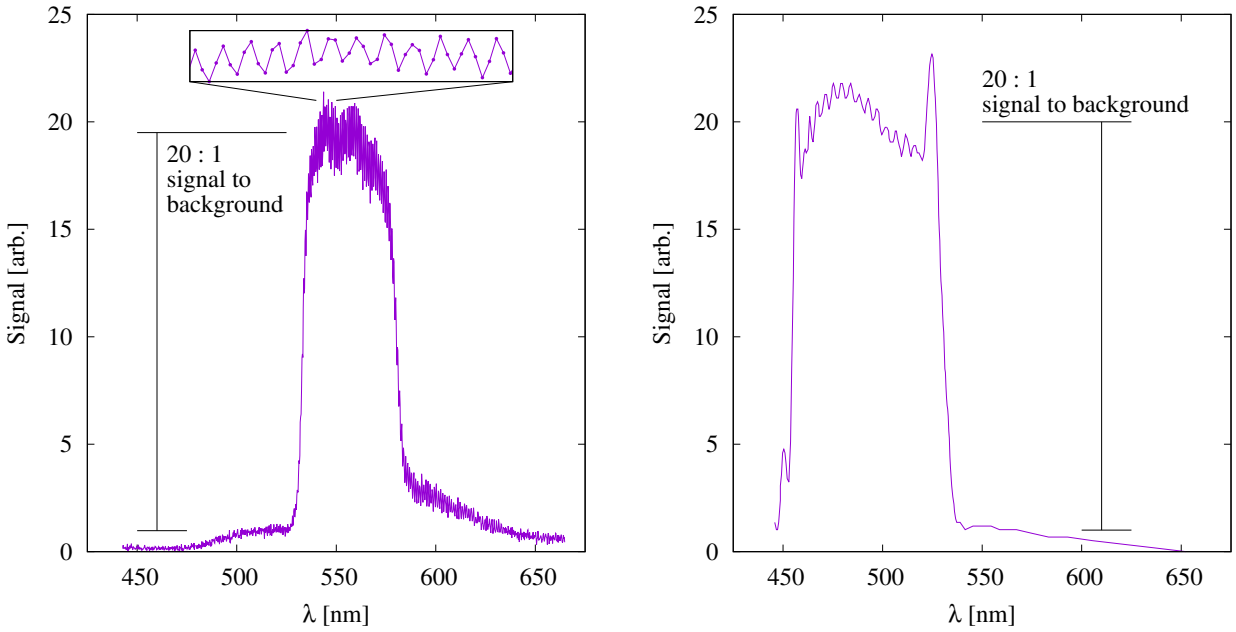

Figure 4: Preliminary proof-of-concept results for soft x-ray absorption in Ce:YAG (left) and hard x-ray absorption in a liquid water sheet (right).

high a continuum generation efficiency as possible. Maximizing the intensity will increase the interferometric sensitivity, and this allows us to minimize the required x-ray dose (Req. 1) as well as accommodate x-ray transparent media (Req. 2).

Our preliminary tests show that the x-ray induced phase change rotates 20 times the light level through the crossed $-45°$ polarizer compared to the leakage. In contrast, the non-interferometric signals require reference normalization by an "un-pumped" spectrum to help tease out the typical 10 – 30% signals [10–13]. Our proof of concept experiments shown in Fig. 4 therefore indicate a preliminary 100 fold increase in signal sensitivity, relieving our need for reference normalization. Such increased signal sensitivity directly addresses all three requirements 1, 2, and 3.

We will focus on two classes of new interaction media: fast refreshing liquid samples and novel condensed materials. We will continue our exploration of ultra-thin, $\leq$1 μm, liquid sheets with the LCLS Sample Environment Department and our existing collaboration with the Marangos group of Imperial College, UK. In addition, however, we will explore novel materials such as perovskite films [39] and low-dimensional free-standing monolayers [40, 41] that are both atomically thin and yet highly optically active materials. These may address the deposition problem and x-ray transparency, but we are also interested in finding faster cascade materials.

We plan to adjust the group delay dispersion (GDD) to match the measurement window to the expected jitter improvements of Table 1. Optimizing the spectral support bandwidth by reducing the GDD chirp from the traditional $\sim$2 ps wide measurement window to only 200 fs gives a factor of 10 increase in the spectral support bandwidth available to probe the carrier cascade evolution. Using the same 200 nm broad spectrum to cover only 200 fs of measurement window would give an ideally matched 1 nm/fs support. At this dispersion, a 15 (23) fs cascade time corresponds to a matched 15 (23) nm support bandwidth at 400 (600)

nm central wavelengths respectively. The 30 fs cascade time typical of Si_3N_4 and diamond would be essentially over-supported for all wavelengths shorter than 800 nm and so we seek a material with a factor of 2 faster carrier cascade without experiencing bandwidth limit temporal blurring.

Our motivation for faster cascades and more radiation sensitive materials have led to two new collaborations: one with the long-time expert in carrier cascade modelling, Beata Ziaja-Motyka of DESY/CFEL [32, 33], and another with Dr. Craig Levin of the Division of Nuclear Medicine at Stanford. With the Levin group, we will investigate novel high-Z scintillation crystals to accelerate the carrier cascading process. We will also explore scintillation sample designs that improve the optical sensitivity for high energy but low dose radiation. Not only a potential route to a sub-picosecond time-resolved positron emission tomography (PET) [42, 43], high sensitivity scintillators could also address our signal per dose requirements (Req. 1). We also note that the primary challenge to jitter control and correction at ultrafast electron diffraction facilities is the very same reduced inelastic scattering cross-section for MeV scale electrons. Ultimately, all three projects – LCLS-II timing, time-of-flight-PET development [42, 43], and ultrafast electron diffraction – will equally benefit from the material developments described here.

Data handling is a key challenge for requirement 3 for which we plan to use a programmable region of interest (ROI) enabled CMOS area detector [44] to read out the cross-polarized spectrum. High speed optical CMOS detectors should allow well above 100 kHz duty-cycle for a 1% ROI readout [45] to be available for FPGA-based algorithms so that data analysis can occur prior to transfer. It is the transfer of the 1% linear ROI and subsequent on-board processing that limits the repetition rate of such a measurement since only the arrival time and quality of measurement need to be transferred to the recording nodes and to the optical laser synchronization system. Only very small data must be transferred over the network to remote data recording nodes. We favor a two-dimensional CMOS detector in order to build the technology around the same detector hardware and optical beam geometries for both the one-dimensional and two-dimensional versions of the interferometric spectral encoding (Objective 2).

For the sake of LCLS-II commissioning in 2019, we will push for a repetition rate that extends beyond the control band of the laser oscillator (requirement 3). A direct measurement of the temporal jitter power spectrum will aid the implementation of synchronization control systems. Furthermore, the tight causal connection between electron bunch and x-ray pulse motivates a direct measurement of the shot-to-shot timing in correlation with high-rate electron bunch diagnostics.

Objective 2 – Attosecond jitter sorting

Attosecond level synchronization is an important extension to interferometric spectral encoding at LCLS-II. One of the biggest challenges for the attosecond science community today is the difficulty in producing significant pulse energy in the 200 eV – 2 keV regime using high harmonic generation (HHG) [19, 20]. Given the importance of understanding exciton flow in photo-excited systems, one can foresee the desire to optically drive electrons into concerted coherent motion [46, 47] and then probe the local electronic environment with e.g. time-resolved resonant inelastic x-ray scattering (tr-RIXS). There have been numerous schemes proposed for developing the attosecond capability of x-ray FEL facilities [21, 22]

with a particular push funded directly by the Office of Basic Energy Science aimed at LCLS-II implementation [30, 48]. The primary obstacle that detracts the attosecond community from using an xFEL source is the lack of intrinsic synchronization enjoyed in lower-fluence lab-based HHG sources.

We propose to investigate a near *in situ* interferometric version of spectrogram encoding, a hybrid of spectral and spatial encoding [23], to achieve 100 attosecond level delay resolution. By crossing the chirped continuum beam relative to the x-ray beam in the material, we obtain a spatially-encoded arrival time in addition to the spectrally-encoded arrival time (Fig. 5, spatial=vertical and spectral=horizontal). Multiple one-dimensional lineouts provide redundant measurements of the arrival time, e.g. spectrally multiplexing the spatially encoded timing signal or vice versa. Related to techniques used in de-noising images [49–52], the multiplexing provides an effective $\sqrt{N}$ improvement in the signal fidelity and thus a more accurately located edge. This multiplexing makes for a more demanding sensitivity requirement than for the one dimensional system. We will need to spread that original few pixel wide signal across the spatial dimension of the spectrograph to cover a few hundred pixel wide region. In order to gain a factor of 10 in temporal resolution, one must multiplex in one of the two dimensions by a factor of 100. This requires a 100 fold increase in signal compared to normal spectral encoding. Here again interferometric sensitivity will help.

Unlike the original crossed-beam implementation, we prefer a tunable temporal window that does not require angle or spot size changes. By using a tilted pulse front rather than crossed beams, we preserve the optical geometry of the one-dimensional version while enabling a tunable measurement window. In addition, we also relieve the coupling of interaction time due to fluctuations in films or liquid sheets. In a crossed beam geometry, if a liquid sheet develops a wobble or if the x-ray pulses induce film vibrations, longitudinal motion of the sample would effectively shift the space-to-time mapping from shot-to-shot. This effect worsens the further one goes away from co-propagating beams. A tilted wave-front in near co-propagating geometry alleviates this problem while still providing a space-to-time mapping that is in fact tunable.

In the tilted pulse-front supercontinuum beam, the pulse envelope experiences a delay across the transverse profile of the beam, indicated schematically in the vertical dimension in Fig. 5 (left). Exactly as in Objective 1, the two crossed polarizations experience a birefringent delay before interacting with an x-ray pulse. After the x-ray interaction, the polarizations are re-timed with a matched birefringent plate, and the signal is read out through the null port of the analyzing polarizer. The resulting diagonal feature in Fig. 5 (right) is then immune to the vertical and horizontal spatial modulations typical of the x-ray transverse profile.

We will leverage high-speed CMOS area detectors to accommodate both the feedback signal for the synchronization system as well as a dynamic region of interest (ROI) selection for attosecond level post-sorting of the residual uncontrolled jitter. Single CMOS lineouts, indicated in Fig. 5 (right) by the purple and green colored lines are projected onto the spectral and spatial axes respectively. These can be immediately read out at well above 100 kHz [45] to determine the one-dimensional edge location for the synchronization system and also the center of the diagonal feature in Fig. 5 (right). This feature covers only about 10% of the full image and so a small set of pixel values need to be read into the image buffer. The shape of that ROI remains constant from shot-to-shot and only its offset will jitter. One gains the multiplexing benefit of the two-dimensional readout even though only $\leq$10% of the full image is passed to the analysis layer. From the current state of the art in CMOS readout — 1 MPix at 1 k frames-per-second [45] — we estimate that we can pull the 10% ROI into the on-board

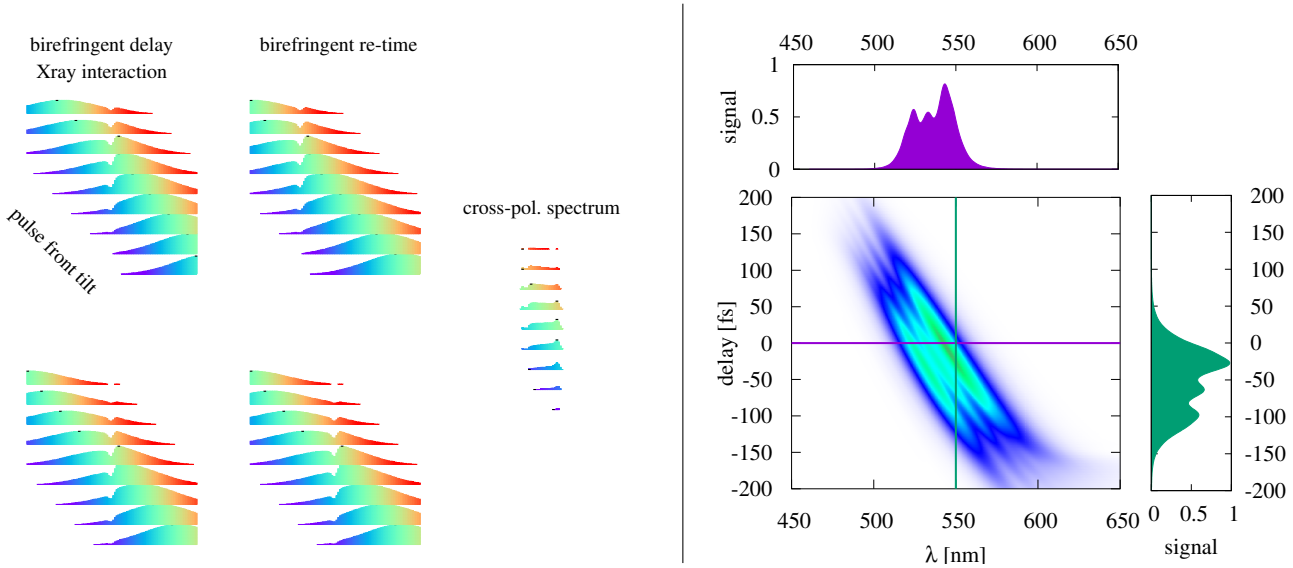

Figure 5: Cartoon (left) and simulation (right) of the two-dimensional interferometric spectrogram concept. Single line-out projections are indicated with line/fill colors.

analysis layer at about 10k fps. Furthermore, we will explore the use of an out-line only ROI that might further reduce the required transfer to the analysis layer and therefore push the 100 attoseconds resolution measurement above 10 kHz. In this way, the same detected signal that provides few femtosecond synchronization control also gives a value that can be used for 100 attoseconds temporal resolution in post sorting of the residual jitter.

With the goal of pushing the attosecond resolution to the full LCLS-II beam rate, we will explore a method known as compressed sensing [49–53]. In compressed sensing, signals that vary in response to a set of under-sampled variable parameters can be effectively interpolated to higher sampling. The requirement is that there exists a representation space, like a rotated Hilbert space, where the variations are sparsely represented. The simplistic example would be if the delay at LCLS-II "jittered" due to a 100 kHz oscillation. Under-sampling that oscillation, quasi-randomly, but on average only at 20 kHz, would require interpolation to predict the arrival times for interstitial pulses. The compressed sensing algorithm would in this case discover that the Fourier basis is the most sparse representation within which all the variation is explained by a 100 kHz δ-function. Thus all of the 930 kHz shots can be "interpolated" *a posteriori*. In practice, the active variables will span multiple dimensions of electron beam energy, orbit, and other parameters, since such algorithms typically work better with high-dimensional initial representations. In fact, this further motivates our highest repetition rate characterization of the delay correlations with electron beam properties mentioned in Objective **??**.

Objective 3 – Attosecond angular streaking

There is increasing momentum in the development of spectro-temporally shaped x-ray FEL pulses [24–30, 54, 55] in response to the rising tide of demand [46, 47, 56–58]. The predominant method to characterize such novel temporal profiles is based on an x-band transverse accelerating cavity (XTCAV) [59] whereby the spent electron bunch is deflected horizontally,

streaked in time by the phase of the transverse accelerating field. A bending magnet then deflects this time-streaked beam vertically proportional to the energy. Imaging the result, one records the time-energy distribution of the spent bunch. This technique has been a critical tool for developing the recent x-ray FEL pulse shaping methods [27, 30]. Unfortunately, it indirectly measures the x-ray temporal profile by identifying the imprint of lasing on the electron bunch. Furthermore, barring a superconducting upgrade to the x-band cavity, the XTCAV can only run at 120 Hz.

Photo-electron streaking, a direct interaction, has the capability to measure the instantaneous temporal structure of x-ray pulses [18]. In photo-electron streaking, a noble gas like neon is dressed by a strong far-infrared or THz field [31,60,61]. As depicted in Fig. 6, the vector potential of the streaking field shifts the outgoing photo-electron energy depending on the phase of the field at the time of photoionization. The temporal shape (purple) can then be read out by the intensity profile of the photo-electrons versus their shifted energies (green), given that the pulse arrives near the zero-crossing of the vector potential. Our recent use of the organic crystal DAST [62] for THz generation was capable of resolving 50 fs separated double pulses of the LCLS [63] that Cavalieri, *et al.* have developed into robust photo-electron streaking system [31]. Such THz and far infrared based schemes [60, 61] have a demanding ∼2 mJ/pulse laser power requirement will likely not scale well for the high repetition rates of LCLS-II (Table 1).

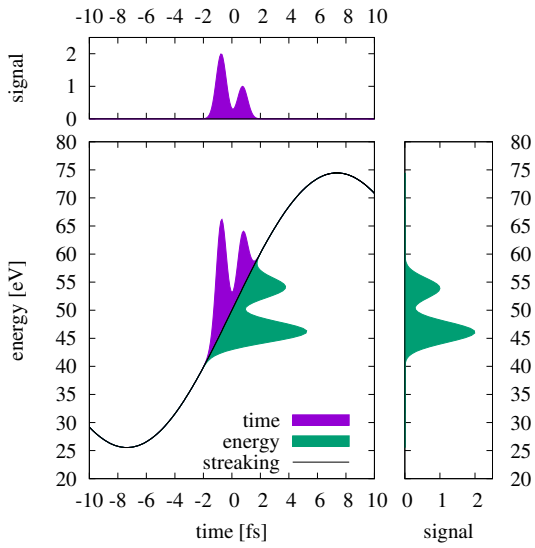

Figure 6: Schematic of linear photo-electron streaking.

The requirement that the x-ray pulse arrive near a zero-crossing of the vector potential is a persistent challenge. The Cavalieri group creatively arranges two photo-electron spectrometers to sample the focal volume of the THz field at two different places across the Gouy phase of the focus. As a beam propagates through a focus it develops a phase advance of π — the Gouy phase — such that one can choose two points just on either side of the focus that have a $\pi/2$ Gouy phase difference. For shots when one of the detectors records the zero crossing of the field, the other detector will measure the maximum kick, thus calibrating the zero-crossing slope. In practice, however, THz and mid-infrared fields depend rather sensitively on environmental factors and on exactly from where in the Gouy phase one measures these streaked photo-electrons. Juranic, *et al.* have attempted to use three spectrometers, one for the unstreaked photo-electron spectrum, and two back-to-back spectrometers to record simultaneously the positively and negatively streaked spectra. This method still suffers when the pulse arrives sufficiently away from the optimal zero-crossing phase.

Miscalibration of the streaking ramp is also common since the changing particulars of the experiment, such as humidity and pump pointing, can dramatically affect the exact shape of the streaking field. For the single cycle THz and few-cycle far-infrared fields typically used in x-ray streaking diagnostics, the fractional bandwidth $\Delta\omega/\omega_0$ is often nearly equal to unity. Such extreme fractional bandwidths make for very irregular carrier fields that vary depending on beam pointing and atmospheric humidity. This is largely why we have chosen

to pursue an alternative approach in Ref. [64].

We will leverage our long history with photo-electron streaking at the LCLS [60, 65, 66] by extending the attosecond angular streaking method of Refs. [67, 68] to the x-ray regime. Pulse-to-pulse variations at an FEL require single-shot measurements much like the velocity map imaging (VMI) [69] extension of attosecond angular streaking [70]. The requirement of a two-dimensional detector, however, likely precludes high repetition rates. We will therefore repurpose what is more traditionally considered an x-ray FEL polarimeter [26, 29, 71, 72] to measure the angularly streaked photo-electron spectra [26, 29, 71, 72].

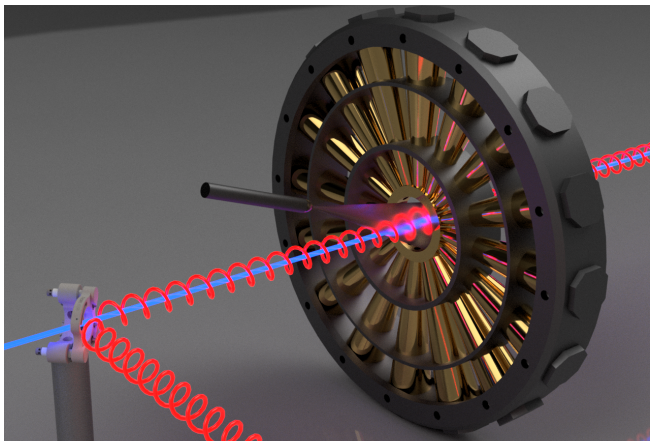

Figure 7: Angular streaking schematic.

We recently demonstrated attosecond angular streaking at LCLS with an angular array of 16 electron time-of-flight detectors — the "CookieBox" — as depicted in Fig. 7. We measured full photo-electron spectra in each of the 16 detectors operating in current, not counting, mode. The result was an x-ray pulse temporal reconstruction with 500 attoseconds resolution [64] which we propose here to extend to the 150 attoseconds resolution scale. We also plan to demonstrate both spectral and polarization sensitivity versus time as well as operation at high repetition rate.

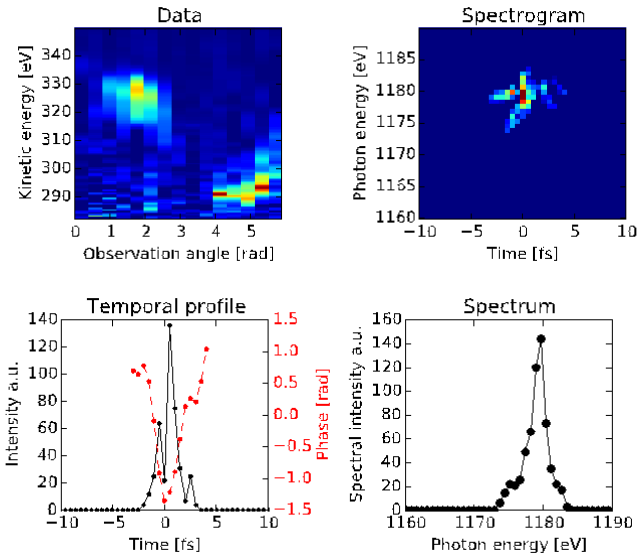

Figure 8: X-ray pulse shape retrieval from our recent angular streaking measurement at LCLS [64].

In angular streaking, the x-ray pulse produces neon photo-electrons that distribute into a dipole probability distribution with a common kinetic energy regardless of emission angle. When dressed with the circularly polarized laser field, shown as the red corkscrew pattern in Fig. 7, those electrons will receive a momentum kick toward the instantaneous direction of the vector potential in a reference frame that spirals relative to the lab frame at the carrier cycle frequency. In this way, one detector will measure electrons with an excess of energy, the opposite detector with less energy, and the two orthogonal detectors will measure the photo-electrons as the projected vector-potential sweeps through a zero-crossing. The additional detectors further constrain the pulse shape retrieval shown in Fig. 8 where the measured spectra reveal a nearly single sub-fs FEL pulse as required for such techniques as impulsive x-ray Raman spectroscopy [58].

Preliminary results demonstrate 500 attoseconds resolution [64]. This resolution depends both on the spectral resolution of the electron time-of-flight spectrometers and on the number of angular sample points per optical cycle. The typical space constraints near

beamlines and individual detector geometries limits the CookieBox array to 16 detectors. Modeled after the original Viefhaus design, we propose a universal main chamber that can accept a micro-channel plate based electron detector with 100 ps impulse response. We have begun discussions with the detector group at University of Bern regarding the design of a modular CookieBox style system. Of particular interest is the application of super-resolution concepts, such as explored for temporal sorting in Objective 2. One generally seeks a non-uniformly distributed under-sampling of a waveform, in this case the angular distribution, in order to reconstruct an accurately interpolated result [49–52]. In simulation we will explore the efficacy of non-uniformly placed detectors for super-resolution in the angular distribution.

We will also shift the dressing laser frequency toward the near-infrared to improve the temporal resolution. Based on Refs. [16, 46, 47] we expect that much of the x-ray pulse characterization needs will lie in the sub-10 fs regime. We propose therefore to shift to a 3 μm wavelength to both improve the fractional bandwidth for a robust carrier shape and to improve the temporal resolution while still preserving an appropriate window for pulse shape retrieval. We expect this change to take our initial demonstration of 500 attosecond resolution for a 10 μm angular streaking field — 33 fs optical cycle — to an expected 150 attoseconds resolution for a 3 μm field — 11 fs optical cycle.

More generally, the angular streaking technique can provide users with a direct measure of novel x-ray pulse shapes as required for stimulated RIXS and other multi-dimensional x-ray spectroscopic techniques [46, 47, 57]. Shown in Fig. 9 we see a simulation of two xFEL pulses, one lower photon energy pulse that is linearly polarized along the horizontal and another higher photon energy pulse that is circularly polarized. From left to right the inter-pulse delay changes from 0 fs – 2 fs. Such a temporal diagnostic will allow not only the demonstration of attosecond FEL pulses but also the full temporal, spectral, and polarization characterization of shaped multi-pulses.

The on-board analysis of the data is a challenging bottleneck in the angular streaking scheme. The raw data in angular streaking is the digitized waveform spanning about 200 ns of record length with a sample frequency of ideally about 4GS/s, one waveform for each of the 16 detectors. All together this would be comparable to a 12.8 kPix image being fed into the analysis layer. We estimate a maximum duty-cycle above 100 kHz by comparing to the 1% CMOS ROI discusses in Objective 1, assuming that the analysis algorithm can

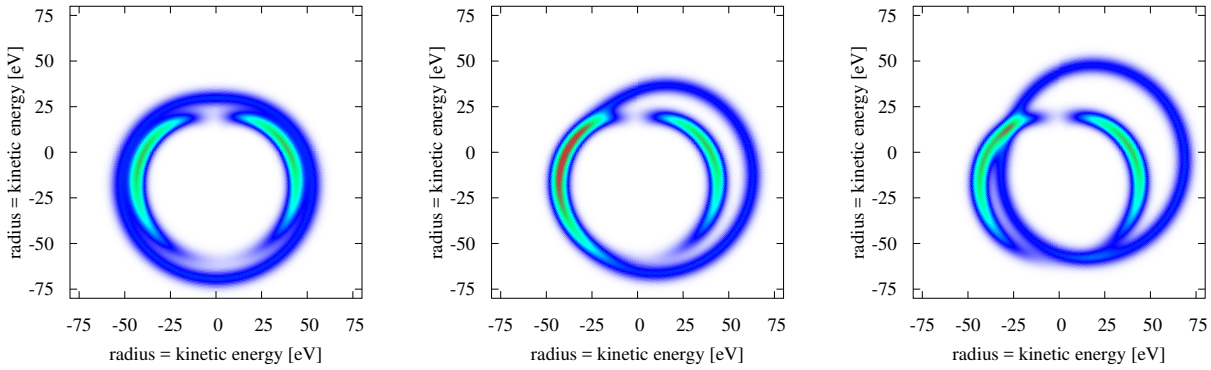

Figure 9: Simulated 3 μm angular streaking as described in the text. From left to right, the inter-pulse delay progresses from 0 fs – 2 fs.

keep up with the data frame rate. Instead of our original iterative retrieval algorithm [64], we plan here to develop a mapping technique that could be implemented as a simple on-board matrix multiplication. In parallel to our pursuit of a mapping algorithm, we will continue our pursuit of machine learning to predict the multi-pulse delays and multi-color separations based only on electron beam information. Through the active collaboration with the Marangos group we have focused initially on using the small data from electron bunch diagnostics as inputs to various machine learning algorithms. [73] The various models are trained based on measured spectra of the final x-ray pulses and the temporal profiles based on XTCAV measurements. After training, the electron bunch diagnostics are used to predict x-ray pulse characteristics such as inter-pulse delay and double pulse separation with 95% or better predictive accuracy (Fig. 10) Ref. [73].

Through another collaboration with the data analysis group at LCLS we are exploring the use of convolutional neural networks for so-called "deep learning." Convolutional neural networks (CNNs) represent the most widely used machine learning architecture for image classification that can also be implemented directly into on-board analysis hardware [74]. We are seeking deep learning methods such as "guided" and "relevance" back propagation to uncover the physical basis of how a neural network determines its predictive outputs [75]. Whether it is a physics based algorithm, a physically interpretable neural network, or simply black-box machine learning, we expect an on-board analysis architecture that will significantly reduce the required data transfer and ideally produce x-ray pulse time-domain waveforms with a duty cycle above 10 kHz.

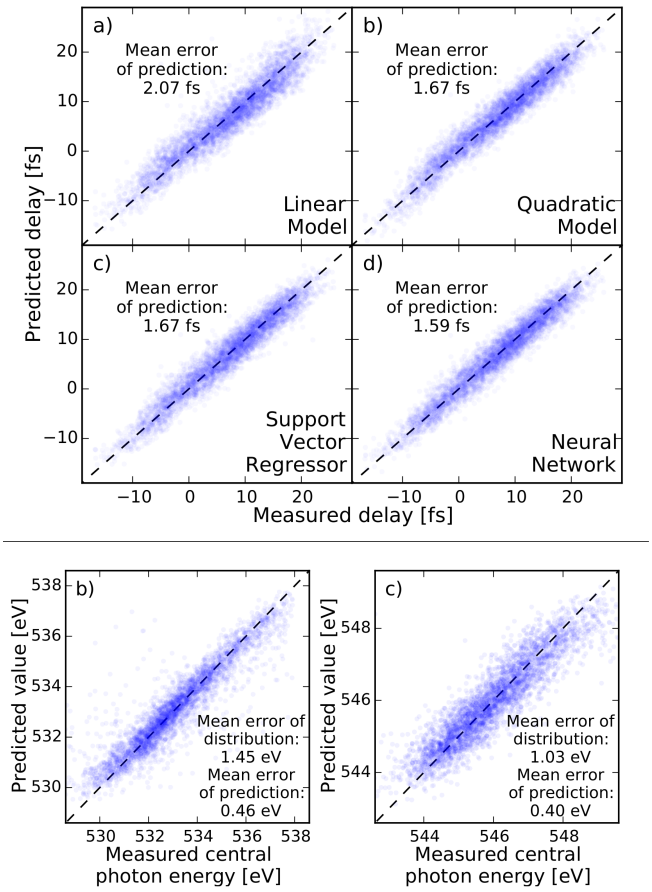

Figure 10: The efficacy of machine learning for predicting temporal delay (top) and color separation (bottom) for shaped FEL pulses. [73]

Organization of Major Activities

We plan to have the base system ready for diagnosing the residual temporal jitter of LCLS-II in advance of the first light in mid-2019. This will allow correlation with the linac and electron bunch parameters and will provide early debugging for the optical synchronization system. The extended system is planned to become available in the early user runs of LCLS-II in 2020 for use in recovering sub-fs single-shot timing. We will benchmark the resolution of the angular streaking method by measuring attosecond and multi-pulse, multi-color, multi-polarization mode of Ref. [29] to benchmark our ability to directly measure the full time-dependent spectrum and polarization of novel shaped x-ray FEL pulses.

Period 1: 7/15/2017 – 7/14/2018, LCLS-I running
Objective 1: Test liquid sheets, graphene, perovskites, and scintillation samples, setup existing 2D opal and Princeton imaging spectrometer, build algorithm based on preliminary data and simulations, acquire 1D array detector and build data acquisition system.
Objective 2: Test birefringence versus pulse-front-tilt and imaging.
Objective 3: Test 3μm streaking with attosecond pulses from LCLS-I using DESY/Viefhaus CookieBox.
Publication(s): "Interferometric Spectral Encoding for high rep-rate FELs"

Period 2: 7/15/2018 – 7/14/2019, LCLS-I down
Objective 1: Finalize the integrated optical system and algorithm and test with water, alcohol series, DMSO, and saline liquid sheets, finalize implementation matrix for various locations in LCLS-II.
Objective 2: Test test liquid sheet signal levels and polarization management, design matched spatial and spectral dispersion, and prototype algorithm dynamic ROI CMOS detection.
Objective 3: Design new CookieBox detector, use existing data to develop physics based algorithms for streaming analysis.
Publication(s): "Femtosecond resolved non-equilibrium, ground electronic state, molecular dynamics in N_2O," and "two-dimensional interferometric spectrogram encoded (2D-ISE) arrival time at high rep-rate FELs."

Period 3: 7/15/2019 – 7/14/2020, LCLS-II commissioning
Objective 1: Commission CMOS lineout system on LCLS-II for synchronization feedback, measure the laser/x-ray jitter power spectrum and correlate with the machine parameters to debug weaknesses, benchmark performance and resolution with N_2O Auger electron spectra versus excited coherent bending and symmetric stretch vibrations.
Objective 2: Integrate dynamic ROI CMOS detector with on-board FPGA or equivalent smart hardware, develop the dynamic ROI algorithm.
Objective 3: Construct new modular CookieBox detector for LCLS-II.
Publication(s): "Optical/x-ray pump-probe resolution at the LCLS-II facility," "Time-domain lock-in amplification of weak interactions at the LCLS-II," and "Novel algorithm for real-time x-ray pulse characterization at the LCLS-II."

Period 4: 7/15/2020 – 7/14/2021, LCLS-II operating
Objective 2: Implement on-board FPGA processing and demonstrate CMOS non-linear ROI masking, build implementation matrix for various locations in LCLS-II.
Objective 3: Build passive CEP locked 3 μm pulses, commission new CookieBox detector for LCLS-II, develop algorithm for streaming analysis, benchmark 150 attosecond resolution.
Publication(s): "Streaming attosecond resolution x-ray pulse characterization: spectrum, polarization, and time." "Optically shaped attosecond x-ray FEL pulses for nonlinear x-ray science"

Period 5: 7/15/2021 – 7/14/2022, LCLS-II operating
Objective 1: Plan extension to hard x-ray regime.
Objective 2: Commission full system with CMOS detector and on-board processing.

Objective 3: Install on LCLS-II with on-board processing, benchmark resolution with NEXAFS of 3 μm laser dressing of N_2O, and develop the implementation matrix for various locations in LCLS-II, and explore high rep-rate application to hard x-ray regime.
Publication(s): "Direct observation of laser-mixing of valence electronic symmetries."

Responsibilities of key project personnel

The PI will be responsible for organizing the major efforts including algorithm development, optical design, and coordination of engineering design and hardware construction. He is expected to contribute 65% of his effort to this project.

The first RA/Project Scientist will be hired at the 75% level with 25% of his or her effort will be shared with closely related Accelerator R&D projects. He or she will work primarily on the optical construction and execution of the experiments in the first two years for the interferometric timing effort. In addition, he or she will organize an initial preliminary benchmark test of attosecond angular streaking based on the Viefhaus CookieBox that will be borrowed from DESY. He or she will begin the effort of designing the CookieBox detector that will be used in the attosecond angular streaking effort. A second RA/Project Scientist will take over the CookieBox detector construction and will lead the attosecond streaking beamtime preparations in years 3-5. He or she will focus also on the optical design and fabrication responsibilities for the final dedicated CookieBox detector and required laser implementation.

We intend to recruit two graduate students from Stanford University to participate in the project. We will seek funding through student research fellowships and LCLS-sponsored student outreach programs. Related research by the PI has attracted numerous externally funded post-doctoral fellows and visiting scientists, most notably Wofram Helml (Marie Curie Foundation), Anton Lidahl (Wallenberg Foundation), and Markus Ilchen (Volkswagen Foundation). We expect these collaborative relasionships to continue. In particular, the close collaboration with the Kienberger Group of TU Munich/MPQ Garching Germany is often financially supported through the Bavaria California Technology Center (BaCaTeC) program [76].

Appendix 1: Biographical Sketch

Ryan Coffee

LCLS Laser Department Tel:650.387.0981
SLAC National Accelerator Laboratory Fax:650.926.2521
Mail Stop 20, Menlo Park, California 94025 E-mail: coffee@slac.stanford.edu

Education and Training

Research Associate		SLAC National Accelerator Laboratory	06/2006–04/2009
Ph.D.	Physics	University of Connecticut	06/2006
M.S.	Physics	University of Connecticut	12/2001
B.S	Physics	University of Arkansas	06/1999
B.A.	Philosophy	University of Arkansas	06/1999

Research and Professional Experience

01/2014–present Staff Scientist, PULSE Institute
04/2009–present Staff Scientist, LCLS Laser Division, SLAC
Spectral and spectrogram encoding of relative x-ray arrival time, sub-10 fs pulse generation for FEL multiplicative seeding and for time resolved photo-chemistry, optical and THz laser streaking techniques at the LCLS, angle-resolved double- and single-core hole spectroscopy of impulsively-aligned molecules, x-ray pump/x-ray probe experiments at LCLS, x-ray pulse shaping for multi-dimensional x-ray spectroscopy, gas phase ultrafast electron diffraction, LCLS experimental laser facility installation and commissioning
06/2006–04/2009 Research Associate, PULSE Institute
Coherent control of rotational wave-packet motion in ambient nitrogen and iodine.
01/2006–06/2006 Research Associate, University of Michigan
Participation in two of the final SPPS experiments
09/1999–06/2006 Research Assistant, Department of Physics, University of Connecticut
Two-color pump-probe optical experiments with nitrogen, molecular vibrational wave-packet motion on laser induced potential energy surfaces, ion time-of-flight spectroscopy, vuv-fluorescence spectroscopy of selective high-order multi-photon absorption in N_2, transient absorption spectroscopy.

Selected publications

1. *Optical Shaping of X-Ray Free-Electron Lasers* A Marinelli, **R Coffee**, *et al.* Physical Review Letters, **116**, 254801 (2016)
2. *Polarization control in an X-ray free-electron laser* AA Lutman . . . **R Coffee**, *et al.* Nature Photonics, **10**, 468 (2016)
3. *Generating femtosecond X-ray pulses using an emittance-spoiling foil in free-electron lasers* Y Ding, C Behrens, **R Coffee**, *et al.* Applied Physics Letters **107**, 191104 (2015)
4. *High-intensity double-pulse X-ray free-electron laser* A Marinelli, . . . **R Coffee**, *et al.* Nature Communications **6**, 6369 (2015)

5. *Measuring the temporal structure of few-femtosecond FEL X-ray pulses directly in the time domain* W Helml, . . . **R Coffee**, *et al.* Nature Photonics, **8**, 950 (2014)
6. *Sub-femtosecond precision measurement of relative X-ray arrival time for free-electron lasers* N Hartmann„ *et al.* **RN Coffee** Nature Photonics **8**, 706 (2014)
7. *Spectral encoding method for measuring the relative arrival time between x-ray/optical pulses* M Bionta, *et al.* **R Coffee** Review of Scientific Instruments, **85**, 083116 (2014)
8. *Multicolor Operation and Spectral Control in a Gain-Modulated X-Ray Free-Electron Laser* A Marinelli„ *et al.* . . . **RN Coffee**, and C Pellegrini Physical Review Letters **111**, 134801 (2013)
9. *Experimental demonstration of femtosecond two-color x-ray free-electron lasers* AA Lutman, R Coffee, *et al.* Physical Review Letters **110**, 134801 (2013)
10. *Spectral encoding of x-ray/optical relative delay* Mina R. Bionta„ *et al.* **R. N. Coffee** Optics Express, **19**, 21855 (2011)

Synergistic Activities

Ultrafast electron diffraction (UED) The PI has recently become intimately involved with the use of ultrafast electron diffraction (UED) in order to merge spectroscopic studies at the LCLS with the structural sensitivity of electron diffraction [77, 78]. The merger of the two experimental paradigms is enabled by induced time-domain coherent molecular motions that in-turn produce concerted fluctuations in both x-ray spectra and in electron diffraction features. By pattern recognizing these common-mode fluctuations, one can merge experimental results as if the two experiments were performed simultaneously. The PI is therefore keenly attuned to need for exquisite synchronization at high energy ultrafast electron diffraction sources. The successful outcome of Objective 1 would be immediately applicable to high energy electron diffraction facilities.

Deep ultra-violet During period two, the LCLS facility will be down. Here we will draw on our existing research program investigating routes to broad-band tunable deep uv. This collaborative work together with the Keinberger group of TU Munich produced a Marie-Curie Fellowship project of Wolfram Helml to develop ultra-broadband, sub-10 fs duration deep ultraviolet pulses. This project later led to a Masters student research project of Patrick Rupprecht to develop the required pulse characterization in the deep uv regime. This deep ultraviolet will be used as a surrogate for the x-ray pulse during the LCLS down time from August 2018 – August 2019. This existing setup will continue to serve as a surrogate source for testing and debugging new concepts and materials.

List of collaborators and co-authors: (48 months)

Collaborators:

Lorenzo Avaldi	CNR-ISM, Rome	Martin Centurion	U. Nebraska,
Nora Berrah	Univ. of Connecticut	Tilo Doeppner	LLNL
Martin Beye	HZB Berlin	Gilles Doumy	ANL
Christoph Bostedt	ANL	Stefan Düsterer	FLASH DESY Hamburg
Marco Cammarata	Univ. of Rennes, France	Raimund Feifel	Univ. of Gothenburg, Sweden
Adrian Cavalieri	CFEL Hamburg	Thomas Fennel	Univ. Rostock, Germany Thomas

Feurer	Univ. of Bern, Switzerland	Serguei Molodtsov	Euro XFEL, Hamburg
Thornton Glover	Gordon & Betty Moore Found.	Anders Nilsson	Uppsala University, Sweden
Jan Grünert	Euro. XFEL, Hamburg	Steve Pratt	ANL
Markus Gühr	Potsdam University, Germany	Artem Rudenko	Kansas State University
Marion Harmand	IMPMC-UPMC, Paris, France	Daniel Rolles	Kansas State University
Janos Hajdu	Uppsala Univ. Sweden	Nina Rohringer	U. of Hamburg, Germany
Christoph Hauri	SwissFEL PSI, Switzerland	Arnaud Rouzee	MBI Berlin
Dan Kane	Mesa Photonics, Albequerque	Ilme Schlichting	MPI Heidelberg
Reinhard Kienberger	TU Munich	Sharon Shwartz	Bar-Ilan University, Israel
Jochen Küpper	CFEL, Hamburg	Klaus Sokolowski-Tinten	U. of Duisburg-Essen, Essen Germany
Jerry LaRue	Chapman, Irvine CA		
Jon Marangos	Imperial College, UK	Thomas Tschentscher	Euro. XFEL Hamburg
Marc Messerschmidt	BioXFEL, Hamburg	Kiyoshi Ueda	Tohoku Univ., Japan
Michael Meyer	Euro. XFEL, Hamburg	Joachim Ullrich	PTB Germany
Catalin Miron	ELI-Delivery Consortium	Jens Viefhaus	DESY
Thomas Möller	TU Berlin		

Graduate and Postdoctoral Advisors

G. Gibson (University of Connecticut), P.H. Bucksbaum (PULSE/Stanford)

Appendix 2: Current and Pending Support

Both current and pending support will be covered under the U.S. Department of Energy / Stanford University Contract for Management and Operation of SLAC National Accelerator Laboratory.

Current Support	LCLS-Laser Science & Technology	100%
Pending support	LCLS-Laser Science & Technology	35%
if awarded Early Career grant	Early Career Award	65%

Appendix 3: Bibliography and References Cited

References

[1] D. M. Fritz, D. A. Reis, B. Adams, R. A. Akre, J. Arthur, C. Blome, P. H. Bucksbaum, A. L. Cavalieri, S. Engemann, S. Fahy, R. W. Falcone, P. H. Fuoss, K. J. Gaffney, M. J. George, J. Hajdu, M. P. Hertlein, P. B. Hillyard, M. Horn von Hoegen, M. Kammler, J. Kaspar, R. Kienberger, P. Krejcik, S. H. Lee, A. M. Lindenberg, B. McFarland, D. Meyer, T. Montagne, É. D. Murray, A. J. Nelson, M. Nicoul, R. Pahl, J. Rudati, H. Schlarb, D. P. Siddons, K. Sokolowski-Tinten, Th. Tschentscher, D. von der Linde, , and J. B. Hastings. Ultrafast bond softening in bismuth: mapping a solid's interatomic potential with x-rays. *Science*, 315:633, February 2007.

[2] T. Katayama, T. Anniyev, M. Beye, R. Coffee, M. DellâĂŹAngela, A. Föhlisch, J. Gladh, S. Kaya, O. Krupin, A. Nilsson, D. Nordlund, W.F. Schlotter, J.A. Sellberg, F. Sorgenfrei, J.J. Turner, W. Wurth, H. Öström, and H. Ogasawara. Ultrafast soft x-ray emission spectroscopy of surface adsorbates using an x-ray free electron laser. *Journal of Electron Spectroscopy and Related Phenomena*, 187(0):9, 2013.

[3] M. Trigo, M. Fuchs, J. Chen, M. P. Jiang, M. Cammarata, S. Fahy, D. M. Fritz, K. Gaffney, S. Ghimire, A. Higginbotham, S. L. Johnson, M. E. Kozina, J. Larsson, H. Lemke, A. M. Lindenberg, G. Ndabashimiye, F. Quirin, K. Sokolowski-Tinten, C. Uher, G. Wang, J. S. Wark, D. Zhu, and D. A. Reis. Fourier-transform inelastic x-ray scattering from time- and momentum-dependent phonon-phonon correlations. *Nat. Phys.*, 9:790, 2013.

[4] B. K. McFarland, J. P. Farrell, S. Miyabe, F. Tarantelli, A. Aguilar, N. Berrah, C. Bostedt, J. D. Bozek, P. H. Bucksbaum, J. C. Castagna, R. N. Coffee, J. P. Cryan, L. Fang, R. Feifel, K. J. Gaffney, J. M. Glownia, T. J. Martinez, M. Mucke, B. Murphy, A. Natan, T. Osipov, V. S. Petrović, S. Schorb, Th. Schultz, L. S. Spector, M. Swiggers, I. Tenney, S. Wang, J. L. White, W. White, and M. Gühr. Ultrafast x-ray auger probing of photoexcited molecular dynamics. *Nat. Commun.*, 5:4235, 2014/06/23/online.

[5] A. L. Cavalieri, D. M. Fritz, S. H. Lee, P. H. Bucksbaum, D. A. Reis, J. Rudati, D. M. Mills, P. H. Fuoss, G. B. Stephenson, C. C. Kao, D. P. Siddons, D. P. Lowney, A. G. MacPhee, D. Weinstein, R. W. Falcone, R. Pahl, J. Als-Nielsen, C. Blome, S. Düsterer, R. Ischebeck, H. Schlarb, H. Schulte-Schrepping, Th. Tschentscher, J. Schneider, O. Hignette, F. Sette, K. Sokolowski-Tinten, H. N. Chapman, R. W. Lee, T. N. Hansen, O. Synnergren, J. Larsson, S. Techert, J. Sheppard, J. S. Wark, M. Bergh, C. Caleman, G. Huldt, D. van der Spoel, N. Timneanu, J. Hajdu, R. A. Akre, E. Bong, P. Emma, P. Krejcik, J. Arthur, S. Brennan, K. J. Gaffney, A. M. Lindenberg, K. Luening, and J. B. Hastings. Clocking femtosecond x rays. *Phys. Rev. Lett.*, 94:114801, Mar 2005.

[6] Cornelius Gahl, Armin Azima, Martin Beye, Martin Deppe, Kristian Döbrich, Urs Hasslinger, Franz Hennies, Alexej Melnikov, Mitsuru Nagasono, Annette Pietzsch, Martin Wolf, Wilfried Wurth, and Alexander Föhlisch. A femtosecond x-ray/optical cross-correlator. *Nature Photonics*, 2:165, 2008.

[7] T. Maltezopoulos, S. Cunovic, M. Wieland, M. Beye, A. Azima, H. Redlin, M. Krikunova, R. Kalms, U. Frühling, F. Budzyn, W. Wurth, A. Föhlisch, and M. Drescher. Single-shot timing measurement of extreme-ultraviolet free-electron laser pulses. *New Journal of Physics*, 10(3):033026, March 2008.

[8] M. Beye, O. Krupin, G. Hays, A. H. Reid, D. Rupp, S. de Jong, S. Lee, W.-S. Lee, Y.-D. Chuang, R. Coffee, J. P. Cryan, J. M. Glownia, A. Fohlisch, M. R. Holmes, A. R. Fry, W. E. White, C. Bostedt, A. O. Scherz, H. A. Durr, and W. F. Schlotter. X-ray pulse preserving single-shot optical cross-correlation method for improved experimental temporal resolution. *Applied Physics Letters*, 100(12):121108, 2012.

[9] S. Schorb, T. Gorkhover, J. P. Cryan, J. M. Glownia, M. R. Bionta, R. N. Coffee, B. Erk, R. Boll, C. Schmidt, D. Rolles, A. Rudenko, A. Rouzee, M. Swiggers, S. Carron, J.-C. Castagna, J. D. Bozek, M. Messerschmidt, W. F. Schlotter, and C. Bostedt. X-ray–optical cross-correlator for gas-phase experiments at the linac coherent light source free-electron laser. *Applied Physics Letters*, 100(12):121107, 2012.

[10] Mina R. Bionta, H. T. Lemke, J. P. Cryan, J. M. Glownia, C. Bostedt, M. Cammarata, J.-C. Castagna, Y. Ding, D. M. Fritz, A. R. Fry, J. Krzywinski, M. Messerschmidt, S. Schorb, M. L. Swiggers, and R. N. Coffee. Spectral encoding of x-ray/optical relative delay. *Opt. Express*, 19(22):21855–21865, Oct 2011.

[11] M. Harmand, R. Coffee, M. R. Bionta, M. Chollet, D. French, D. M. Fritz, H. Lemke, N. Medvedev, B. Ziaja, S. Toleikis, and M. Cammarata. Achieving few-femtosecond time-sorting at hard x-ray free electron lasers. *Nat. Phot.*, 7:215, 2013.

[12] *Femtosecond optical/hard X-ray timing diagnostics at an FEL: implementation and performance*, volume 8778, 2013.

[13] M. R. Bionta, N. Hartmann, M. Weaver, D. French, D. J. Nicholson, J. P. Cryan, J. M. Glownia, K. Baker, C. Bostedt, M. Chollet, Y. Ding, D. M. Fritz, A. R. Fry, D. J. Kane, J. Krzywinski, H. T. Lemke, M. Messerschmidt, S. Schorb, D. Zhu, W. E. White, and R. N. Coffee. Spectral encoding method for measuring the relative arrival time between x-ray/optical pulses. *Review of Scientific Instruments*, 85(8):083116, 2014.

[14] Tadashi Togashi, Takahiro Sato, Kanade Ogawa, Tetsuo Katayama, Shigeki Owada, Yuichi Inubushi, Kensuke Tono, and Makina Yabashi. Arrival-timing diagnostics for pump-probe experiments in sacla, using x-ray-induced optical transparency in gaas. In *19th International Conference on Ultrafast Phenomena*, page 07.Mon.P1.51. Optical Society of America, 2014.

[15] Tetsuo Katayama, Shigeki Owada, Tadashi Togashi, Kanade Ogawa, Petri Karvinen, Ismo Vartiainen, Anni Eronen, Christian David, Takahiro Sato, Kyo Nakajima, Yasumasa Joti, Hirokatsu Yumoto, Haruhiko Ohashi, and Makina Yabashi. A beam branching method for timing and spectral characterization of hard x-ray free-electron lasers. *Structural Dynamics*, 3(3), 2016.

[16] R.W. Schoenlein *et al.* New science opportunities enabled by lcls-ii x-ray lasers. *SLAC Report*, pages SLAC–R–1053, 2015.

[17] M. Lewenstein, Ph. Balcou, M. Yu. Ivanov, Anne L'Huillier, and P. B. Corkum. Theory of high-harmonic generation by low-frequency laser fields. *Phys. Rev. A*, 49:2117–2132, Mar 1994.

[18] M. Hentschel, R. Kienberger, Ch. Spielmann, G. A. Reider, N. Milosevic, T. Brabec, P. Corkum, U. Heinzmann, M. Drescher, and F. Krausz. Attosecond metrology. *Nature*, 414:509, 2001.

[19] Ming-Chang Chen, Christopher Mancuso, Carlos HernÃąndez-GarcÃŋa, Franklin Dollar, Ben Galloway, Dimitar Popmintchev, Pei-Chi Huang, Barry Walker, Luis Plaja, Agnieszka A. JaroÅĎ-Becker, Andreas Becker, Margaret M. Murnane, Henry C. Kapteyn, and Tenio Popmintchev. Generation of bright isolated attosecond soft x-ray pulses driven by multicycle midinfrared lasers. *Proceedings of the National Academy of Sciences*, 111(23):E2361–E2367, 2014.

[20] Bruno E. Schmidt, Nicolas Thiré, Vincent Cardin, Samuel Beaulieu, Vincent Wanie, Matteo Negro, Caterina Vozzi, Valer Tosa, and François Légaré. Single shot absorption measurements in the water window xuv region via hhg. In *High-Brightness Sources and Light-Driven Interactions*, page HT2B.1. Optical Society of America, 2016.

[21] Y. Ding, Z. Huang, D. Ratner, P. Bucksbaum, and H. Merdji. Generation of attosecond x-ray pulses with a multicycle two-color enhanced self-amplified spontaneous emission scheme. *Phys. Rev. ST Accel. Beams*, 12:060703, Jun 2009.

[22] D. Xiang, Z. Huang, and G. Stupakov. Generation of intense attosecond x-ray pulses using ultraviolet laser induced microbunching in electron beams. *Phys. Rev. ST Accel. Beams*, 12:060701, Jun 2009.

[23] Hartmann N. and Helml W. and Galler A. and Bionta M. R. Grünert J. and Molodtsov S. and Ferguson K. R. and Schorb S. and Swiggers M. L. and Carron S. and Bostedt C. and Castagna J.-C. and Bozek J. and Glownia J. M. and Kane D. J. and Fry A. R. and White W. E. and Hauri C. P. and Feurer T. and Coffee R. N. Sub-femtosecond precision measurement of relative x-ray arrival time for free-electron lasers. *Nat. Photon.*, 8:706, 7 2014.

[24] A. A. Lutman, R. Coffee, Y. Ding, Z. Huang, J. Krzywinski, T. Maxwell, M. Messerschmidt, and H.-D. Nuhn. Experimental demonstration of femtosecond two-color x-ray free-electron lasers. *Phys. Rev. Lett.*, 110:134801, Mar 2013.

[25] A. Marinelli, A. A. Lutman, J. Wu, Y. Ding, J. Krzywinski, H.-D. Nuhn, Y. Feng, R. N. Coffee, and C. Pellegrini. Multicolor operation and spectral control in a gain-modulated x-ray free-electron laser. *Phys. Rev. Lett.*, 111:134801, Sep 2013.

[26] Enrico Allaria, Bruno Diviacco, Carlo Callegari, Paola Finetti, Benoît Mahieu, Jens Viefhaus, Marco Zangrando, Giovanni De Ninno, Guillaume Lambert, Eugenio Ferrari, Jens Buck, Markus Ilchen, Boris Vodungbo, Nicola Mahne, Cristian Svetina, Carlo Spezzani, Simone Di Mitri, Giuseppe Penco, Mauro Trovó, William M. Fawley, Primoz R. Rebernik, David Gauthier, Cesare Grazioli, Marcello Coreno, Barbara Ressel, Antti Kivimäki, Tommaso Mazza, Leif Glaser, Frank Scholz, Joern Seltmann, Patrick Gessler, Jan Grünert, Alberto De Fanis, Michael Meyer, André Knie, Stefan P. Moeller,

Lorenzo Raimondi, Flavio Capotondi, Emanuele Pedersoli, Oksana Plekan, Miltcho B. Danailov, Alexander Demidovich, Ivaylo Nikolov, Alessandro Abrami, Julien Gautier, Jan Lüning, Philippe Zeitoun, and Luca Giannessi. Control of the polarization of a vacuum-ultraviolet, high-gain, free-electron laser. *Phys. Rev. X*, 4:041040, Dec 2014.

[27] A. Marinelli, D. Ratner, J. Lutman, A.A. Turner, J. Welch, F.-J. Decker, H. Loos, C. Behrens, S. Gilevich, A.A. Miahnahri, S. Vetter, T.J. Maxwell, Y. Ding, R. Coffee, S. Wakatsuki, and Z. Huang. High-intensity double-pulse x-ray free-electron laser. *Nat. Commun.*, 6:6369, 2015.

[28] Prince K. C., Allaria E., Callegari C., Cucini R., De Ninno G., Di Mitri S., Diviacco B., Ferrari E., Finetti P., Gauthier D., Giannessi L., Mahne N., Penco G., Plekan O., Raimondi L., Rebernik P., Roussel E., Svetina C., TrovÃš M., Zangrando M., Negro M., Carpeggiani P., Reduzzi M., Sansone G., Grum-Grzhimailo A. N., Gryzlova E. V., Strakhova S. I., Bartschat K., Douguet N., Venzke J., Iablonskyi D., Kumagai Y., Takanashi T., Ueda K., Fischer A., Coreno M., Stienkemeier F., Ovcharenko Y., Mazza T., and Meyer M. Coherent control with a short-wavelength free-electron laser. *Nat. Photon.*, 10:176, 2016.

[29] Alberto A. Lutman, James P. MacArthur, Markus Ilchen, Anton O. Lindahl, Jens Buck, Ryan N. Coffee, Georgi L. Dakovski, Lars Dammann, Yuantao Ding, Hermann A. DÃijrr, Leif Glaser, Jan GrÃijnert, Gregor Hartmann, Nick Hartmann, Daniel Higley, Konstantin Hirsch, Yurii I. Levashov, Agostino Marinelli, Tim Maxwell, Ankush Mitra, Stefan Moeller, Timur Osipov, Franz Peters, Marc Planas, Ivan Shevchuk, William F. Schlotter, Frank Scholz, JÃűrn Seltmann, Jens Viefhaus, Peter Walter, Zachary R. Wolf, Zhirong Huang, and Heinz-Dieter Nuhn. Polarization control in an x-ray free-electron laser. *Nat. Photon.*, 10:468–472, 2016.

[30] A. Marinelli, R. Coffee, S. Vetter, P. Hering, G. N. West, S. Gilevich, A. A. Lutman, S. Li, T. Maxwell, J. Galayda, A. Fry, and Z. Huang. Optical shaping of x-ray free-electron lasers. *Phys. Rev. Lett.*, 116:254801, Jun 2016.

[31] S. Schulz, I. GrguraÅą, C. Behrens, H. Bromberger, J. T. Costello, M. K. Czwalinna, M. Felber, M. C. Hoffmann, M. Ilchen, H. Y. Liu, T. Mazza, M. Meyer, S. Pfeiffer, P. PrÄŹdki, S. Schefer, C. Schmidt, U. Wegner, H. Schlarb, and A. L. Cavalieri. Femtosecond all-optical synchronization of an x-ray free-electron laser. *Nat. Commun.*, page 5938, 2015.

[32] Beata Ziaja, Richard A. London, and Janos Hajdu. Unified model of secondary electron cascades in diamond. *Journal of Applied Physics*, 97(6), 2005.

[33] Chun Hongx Yoon, Mikhail V. Yurkov, Evgeny A. Schneidmiller, Liubov Samoylova, Alexey Buzmakov, Zoltan Jurek, Beata Ziaja, Robin Santra, N. Duane Loh, Thomas Tschentscher, and Adrian P. Mancuso. A comprehensive simulation framework for imaging single particles and biomolecules at the european x-ray free-electron laser. *Sci. Reps.*, 6:24791, 2016.

[34] O. Krupin, M. Trigo, W. F. Schlotter, M. Beye, F. Sorgenfrei, J. J. Turner, D. A. Reis, N. Gerken, S. Lee, W. S. Lee, G. Hays, Y. Acremann, B. Abbey, R. Coffee, M. Messerschmidt, S. P. Hau-Riege, G. Lapertot, J. Lüning, P. Heimann, R. Soufli, M. Fernández-Perea, M. Rowen, M. Holmes, S. L. Molodtsov, A. Föhlisch, and W. Wurth. Temporal

cross-correlation of x-ray free electron and optical lasers using soft x-ray pulse induced transient reflectivity. *Opt. Express*, 20(10):11396–11406, May 2012.

[35] Reinhard Kienberger. X-ray pulse-measurement by chirped pulse laser assisted auger decay: a letter of intent, 2005.

[36] Y.-H. Chen, S. Varma, I. Alexeev, and H. Milchberg. Measurement of transient nonlinear refractive index in gases using xenon supercontinuum single-shot spectral interferometry. *Opt. Express*, 15(12):7458, Jun 2007.

[37] S. L. Chin, A. Brodeur, S. Petit, O. G. Kosareva, and V. P. Kandidov. Filamentation and supercontinuum generation during the propagation of powerful ultrashort laser pulses in optical media (white light laser). *Journal of Nonlinear Optical Physics & Materials*, 08(01):121–146, 1999.

[38] Yu-Chen Cheng, Chih-Hsuan Lu, Yuan-Yao Lin, and A. H. Kung. Supercontinuum generation in a multi-plate medium. *Opt. Express*, 24(7):7224–7231, Apr 2016.

[39] Adam H. Slavney, Te Hu, Aaron M. Lindenberg, and Hemamala I. Karunadasa. A bismuth-halide double perovskite with long carrier recombination lifetime for photovoltaic applications. *Journal of the American Chemical Society*, 138(7):2138–2141, 2016. PMID: 26853379.

[40] Kin Fai Mak, Changgu Lee, James Hone, Jie Shan, and Tony F. Heinz. Atomically thin mos_2: A new direct-gap semiconductor. *Phys. Rev. Lett.*, 105:136805, Sep 2010.

[41] Chun Hung Lui, Kin Fai Mak, Jie Shan, and Tony F. Heinz. Ultrafast photoluminescence from graphene. *Phys. Rev. Lett.*, 105:127404, Sep 2010.

[42] Craig S Levin. Advanced time-of-flight (tof) pet photon detectors. `http://miil.stanford.edu/research/tofdetector.html`.

[43] Virginia Ch. Spanoudaki and Craig S. Levin. Photo-detectors for time of flight positron emission tomography (tof-pet). *Sensors*, 10(11):10484, 2010.

[44] Noil2sm1300a – lupa1300-2: High speed cmos image sensor, July 2015. `http://www.onsemi.com/pub_link/Collateral/NOIL2SM1300A-D.PDF`.

[45] Pieter Willems. High speed cmos image sensors. *Planet Analog*, 2007. `http://www.cypress.com/file/88686/download`.

[46] Jason D. Biggs, Yu Zhang, Daniel Healion, and Shaul Mukamel. Two-dimensional stimulated resonance raman spectroscopy of molecules with broadband x-ray pulses. *The Journal of Chemical Physics*, 136(17):174117, 2012.

[47] Shaul Mukamel, Daniel Healion, Yu Zhang, and Jason D. Biggs. Multidimensional attosecond resonant x-ray spectroscopy of molecules: Lessons from the optical regime. *Annual Review of Physical Chemistry*, 64(1):101–127, 2013. PMID: 23245522.

[48] A. Marinelli. Sub-fs pulses from a laser-enhanced x-ray free-electron laser. *DOE BES grant*, 2016.

[49] E. Candes, J. Romberg, and T. Tao. Robust Uncertainty Principles: Exact Signal Reconstruction from Highly Incomplete Frequency Information. *ArXiv Mathematics e-prints*, September 2004.

[50] E. Candes and T. Tao. Near Optimal Signal Recovery From Random Projections: Universal Encoding Strategies? *ArXiv Mathematics e-prints*, October 2004.

[51] E. Candes, J. Romberg, and T. Tao. Stable Signal Recovery from Incomplete and Inaccurate Measurements. *ArXiv Mathematics e-prints*, March 2005.

[52] M. Elad and M. Aharon. Image denoising via sparse and redundant representations over learned dictionaries. *Image Processing, IEEE Transactions on*, 15(12):3736–3745, Dec 2006.

[53] Jordan Ellenberg. Fill in the blanks: using math to turn lo-res datasets into hi-res samples. *Wired*, Feb. 2010.

[54] Dao Xiang and Gennady Stupakov. Echo-enabled harmonic generation free electron laser. *Phys. Rev. ST Accel. Beams*, 12:030702, Mar 2009.

[55] E. Hemsing, M. Dunning, B. Garcia, C. Hast, T. Raubenheimer, G. Stupakov, and D. Xiang. Echo-enabled harmonics up to the 75th order from precisely tailored electron beams. *Nat. Photon.*, 10:512, 2016.

[56] Igor V. Schweigert and Shaul Mukamel. Coherent ultrafast core-hole correlation spectroscopy: X-ray analogues of multidimensional nmr. *Phys. Rev. Lett.*, 99:163001, Oct 2007.

[57] G. Marcus, G. Penn, and A. A. Zholents. Free-electron laser design for four-wave mixing experiments with soft-x-ray pulses. *Phys. Rev. Lett.*, 113:024801, Jul 2014.

[58] S. Miyabe and P. Bucksbaum. Transient impulsive electronic raman redistribution. *Phys. Rev. Lett.*, 114:143005, Apr 2015.

[59] C. Behrens, F.-J. Decker, Y. Ding, V. A. Dolgashev, J. Frisch, Z. Huang, P. Krejcik, H. Loos, A. Lutman, T. J. Maxwell, J. Turner, J. Wang, M.-H. Wang, J. Welch, and J. Wu. Few-femtosecond time-resolved measurements of x-ray free-electron lasers. *Nat. Commun.*, 5:3762, 2014.

[60] Helml W., A. R. Maier, W. Schweinberger, I. Grguraš, P. Radcliffe, G. Doumy, C. Roedig, J. Gagnon, M. Messerschmidt, S. Schorb, C. Bostedt, F. Grüner, L. F. DiMauro, D. Cubaynes, J. D. Bozek, Th. Tschentscher, J. T. Costello, M. Meyer, R. Coffee, S. Düsterer, A. L. Cavalieri, and R. Kienberger. Measuring the temporal structure of few-femtosecond fel x-ray pulses directly in the time domain. *Nat. Photon.*, 8:950–957, 12 2014.

[61] P. N. Juranić, A. Stepanov, R. Ischebeck, V. Schlott, C. Pradervand, L. Patthey, M. Radović, I. Gorgisyan, L. Rivkin, C. P. Hauri, B. Monoszlai, R. Ivanov, P. Peier, J. Liu, T. Togashi, S. Owada, K. Ogawa, T. Katayama, M. Yabashi, and R. Abela. High-precision x-ray fel pulse arrival time measurements at sacla by a thz streak camera with xe clusters. *Opt. Express*, 22(24):30004–30012, Dec 2014.

[62] Arno Schneider, Max Neis, Marcel Stillhart, Blanca Ruiz, Rizwan U. A. Khan, and Peter Günter. Generation of terahertz pulses through optical rectification in organic dast crystals: theory and experiment. *J. Opt. Soc. Am. B*, 23(9):1822–1835, Sep 2006.

[63] M. Hoffmann, *et al.* Femtosecond profiling of shaped x-ray pulses. *in review*.

[64] N. Hartmann, G. Hartmann, R. Heider, M. S. Wagner, M. Ilchen, J. Buck, A. Lindahl, C. Benko, C. Bostedt, J. Gruenert, J. Krzywinski, J. Liu, A. Lutman, A. Marinelli, T. Maxwell, A. Miahnahri, S. Moeller, M. Planas, J. Robinson, J. Viefhaus, T. Feurer, R. Kienberger, R. N. Coffee, , and W. Helml. Attosecond structure of x-ray free-electron laser pulses revealed by angular streaking. *in prep.*

[65] S Düsterer, P Radcliffe, C Bostedt, J Bozek, A L Cavalieri, R Coffee, J T Costello, D Cubaynes, L F DiMauro, Y Ding, G Doumy, F Grüner, W Helml, W Schweinberger, R Kienberger, A R Maier, M Messerschmidt, V Richardson, C Roedig, T Tschentscher, and M Meyer. Femtosecond x-ray pulse length characterization at the linac coherent light source free-electron laser. *New Journal of Physics*, 13(9):093024, 2011.

[66] M. Meyer, P. Radcliffe, T. Tschentscher, J. T. Costello, A. L. Cavalieri, I. Grguras, A. R. Maier, R. Kienberger, J. Bozek, C. Bostedt, S. Schorb, R. Coffee, M. Messerschmidt, C. Roedig, E. Sistrunk, L. F. Di Mauro, G. Doumy, K. Ueda, S. Wada, S. Düsterer, A. K. Kazansky, and N. M. Kabachnik. Angle-resolved electron spectroscopy of laser-assisted auger decay induced by a few-femtosecond x-ray pulse. *Phys. Rev. Lett.*, 108:063007, Feb 2012.

[67] Eric Constant, Vladimir D. Taranukhin, Albert Stolow, and P. B. Corkum. Methods for the measurement of the duration of high-harmonic pulses. *Phys. Rev. A*, 56:3870–3878, Nov 1997.

[68] Petrissa Eckle, Mathias Smolarski, Philip Schlup, Jens Biegert, Andre Staudte, Markus Schoffler, Harm G. Muller, Reinhard Dorner, and Ursula Keller. Attosecond angular streaking. *Nat. Phys.*, 4:565, 2008.

[69] Marc J. J. Vrakking. An iterative procedure for the inversion of two-dimensional ion/photoelectron imaging experiments. *Review of Scientific Instruments*, 72(11):4084–4089, 2001.

[70] Matthias Weger, Jochen Maurer, André Ludwig, Lukas Gallmann, and Ursula Keller. Transferring the attoclock technique to velocity map imaging. *Opt. Express*, 21(19):21981–21990, Sep 2013.

[71] M. Ilchen, L. Glaser, F. Scholz, P. Walter, S. Deinert, A. Rothkirch, J. Seltmann, J. Viefhaus, P. Decleva, B. Langer, A. Knie, A. Ehresmann, O. M. Al-Dossary, M. Braune, G. Hartmann, A. Meissner, L. C. Tribedi, M. AlKhaldi, and U. Becker. Angular momentum sensitive two-center interference. *Phys. Rev. Lett.*, 112:023001, Jan 2014.

[72] T. Mazza, M. Ilchen, A. J. Rafipoor, C. Callegari, P. Finetti, O. Plekan, K. C. Prince, R. Richter, M. B. Danailov, A. Demidovich, G. De Ninno, C. Grazioli, R. Ivanov, N. Mahne, L. Raimondi, C. Svetina, L. Avaldi, P. Bolognesi, M. Coreno, P. O'Keeffe, M. Di Fraia, M. Devetta, Y. Ovcharenko, Th. MÃűller, V. Lyamayev, F. Stienkemeier, S. DÃijsterer,

K. Ueda, J. T. Costello, A. K. Kazansky, N. M. Kabachnik, and M. Meyer. Determining the polarization state of an extreme ultraviolet free-electron laser beam using atomic circular dichroism. *Nat. Commun.*, 5:3648, 2014.

[73] A. Sanchez-Gonzalez, P. Micaelli, C. Olivier, T. R. Barillot, M. Ilchen, A. A. Lutman, A. Marinelli, T. Maxwell, A. Achner, M. AgÃěker, N. Berrah, C. Bostedt, J. Buck, P. H. Bucksbaum, S. Carron Montero, B. Cooper, J. P. Cryan, M. Dong, R. Feifel, L. J. Frasinski, H. Fukuzawa, A. Galler, G. Hartmann, N. Hartmann, W. Helml, A. S. Johnson, A. Knie, A. O. Lindahl, J. Liu, K. Motomura, M. Mucke, C. O'Grady, J-E. Rubensson, E. R. Simpson, R. J. Squibb, C. SÃěthe, K. Ueda, M. Vacher, D. J. Walke, V. Zhaunerchyk, R. N. Coffee, and J. P. Marangos. Machine learning applied to single-shot x-ray diagnostics in an XFEL. *arXiv*, page 1610.03378, 2016.

[74] Expandable cognimem neural network. `http://www.cognimem.com/products/chips-and-modules/CMEnK-Module/index.html`.

[75] Mihir Mongia, David Schneider, and Ryan N. Coffee. An interpretable deep learning algorithm to overcome limited hardware in lcls experiments. *in prep.*

[76] Bavaria california technology center (bacatec). `http://www.bacatec.de/en/index.html`.

[77] S. P. Weathersby, G. Brown, M. Centurion, T. F. Chase, R. Coffee, J. Corbett, J. P. Eichner, J. C. Frisch, A. R. Fry, M. GÃijhr, N. Hartmann, C. Hast, R. Hettel, R. K. Jobe, E. N. Jongewaard, J. R. Lewandowski, R. K. Li, A. M. Lindenberg, I. Makasyuk, J. E. May, D. McCormick, M. N. Nguyen, A. H. Reid, X. Shen, K. Sokolowski-Tinten, T. Vecchione, S. L. Vetter, J. Wu, J. Yang, H. A. DÃijrr, and X. J. Wang. Mega-electron-volt ultrafast electron diffraction at slac national accelerator laboratory. *Review of Scientific Instruments*, 86(7), 2015.

[78] Jie Yang, Markus Guehr, Theodore Vecchione, Matthew S. Robinson, Renkai Li, Nick Hartmann, Xiaozhe Shen, Ryan Coffee, Jeff Corbett, Alan Fry, Kelly Gaffney, Tais Gorkhover, Carsten Hast, Keith Jobe, Igor Makasyuk, Alexander Reid, Joseph Robinson, Sharon Vetter, Fenglin Wang, Stephen Weathersby, Charles Yoneda, Martin Centurion, and Xijie Wang. Diffractive imaging of a rotational wavepacket in nitrogen molecules with femtosecond megaelectronvolt electron pulses. *Nat. Comms.*, 7:11232, 2016.

Appendix 4: Facilities and Other Resources

There are two principle lab spaces identified for this project.

- LCLS-AMO laser system when not in use by user experiments, this is the primary laser for the x-ray spectroscopy arm of this program.
- Laser only based commissioning and development experiments will be carried out in one of the new laser labs in the Photon Science Laboratory Building (PSLB).

Analysis resources exist from both the SLAC-unix farm and the LCLS-unix farms. Our long collaboration with the data analysis and controls groups at LCLS not only allows the PI particularly early insight into the computing resources, but is also motivates his active pursuit of data compression and on-board analysis algorithms. This mutual benefit ensures the continued use and support for these computing facilities.

Office space will be available for all team members in the Laser Division area of building 751 with additional space for students and visiting scientists in the PULSE Institute.

Additional Personnel

As noted above, there will be likely two graduate student recruited from Stanford University who will work on this project. Those students participate via the student outreach programs of LCLS at SLAC.

Appendix 5: Equipment

The primary laser system identified for offline optical work will reside in one of the new laser labs located in the Photon Science Laboratory Building (PSLB) at SLAC. Prior to the occupancy of PSLB, we will focus our efforts on using the AMO laser system at LCLS for both beamtime preparations as well as offline work when not interfering with scheduled user experiments. Required equipment under the general use of the laser division at LCLS are:

- Noble-gas-cell based continuum generation and pulse compression system.
- Visible imaging spectrometer for spectrogram retrieval.
- Data Acquisition System including high frame-rate linear CCD and 2D CMOS cameras

with associated laser systems:

- LCLS-AMO laser system is available when not serving user experiments and during the projected LCLS down times.
- The R&D laser lab in the PSLB will house an amplified Ti:Sapphire laser system similar to the existing LCLS laser systems.
-

Other equipment available to the project include: TOPAS-c 2 for generation of 3 μm pulses.

Appendix 6: Data Management Plan

As stated in the project narrative, one of the central themes is to reduce the data load. The data that is accumulated as part of this project will be made broadly available both internally via SLAC/LCLS unix user account access and, by inquiry to the PI, externally via coordinated data formatting and access FTP.

Data taken with the LCLS will be stored in accordance with LCLS policy also in SLAC Central Storage (or LCLS storage if in future LCLS moves the storage service). Access can then be granted by the PI also for any individual who obtains an LCLS user unix account.

The laser lab based data will be housed in the SLAC Central Computing. The PI currently maintains a 1 TB/year subscription and that will be incrementally increased up to a 5 TB/year storage, expanded when needed. The data will be made broadly available by SLAC unix account access and externally by contacting the PI and coordinating an FTP service of the data.

Appendix 7: Letters of Collaboration

Please see attached Letters of Collaboration.